DC Link approach to Variable-Speed, Sensorless, Induction Motor Drive

Ch.U.Phanendra.Kumar [1]
Asst.Professor ,HOD,LIMAT
contactphanendra@gmail.com

SK.Mohiddin[2]
Asst.Professor, LIMAT
shaik36mohiddin@gmail.com

A.Hanumaiah [3]
Professor,VLITS
appikatlahanumaiah1965@gmail.com

Abstract— **This paper presents a new control strategy for three-phase induction motor which includes independent speed & torque control loops and hence current regulation thereby overcoming the limitation (i.e. sluggish response) of volts per hertz controlled method. For close-loop control, the feedback signals including the rotor speed, flux and torque are not measured directly but are estimated by means of an algorithm. The inputs to this algorithm are the reconstructed waveforms of stator currents and voltages obtained from the dc link indirectly on stator side. The proposed drive thus requires only one sensor in the dc link to implement the close-loop speed and torque control of a three-phase induction motor. The simulation results on a 2.2 kW induction motor drive in Matlab/Simulink software show fast dynamic response and good agreement between the actual values and the estimated values of torque and speed. Replacement of the open-loop control strategy of existing v/f drive by the proposed close-loop strategy appears to be possible without requiring any additional power components and sensors.**

***Index Terms*— Speed-sensorless, estimation, dc link, band-pass filter, reconstruction, three-phase induction motor, space-vector.**

NOMENCLATURE

R_s R_r' Stator and rotor resistances (Ω)

L_m L_r' Magnetizing and rotor inductances (Henry)

I. INTRODUCTION

The widespread industrial use of induction motor (IM) has been stimulated over the years by their relative cheapness, low maintenance and high reliability. The control of IM variable speed drives [1] often requires control of machine currents, which is normally achieved by using a voltage source inverter. A large number of control strategies have been registered so far [2]-[4]. The volts per hertz (v/f) IM drives with inverters are widely used in a number of industrial applications promising not only energy saving, but also improvement in productivity and quality. The low cost applications usually adopt v/f scalar control when no particular performance is required. Variable-speed pumps, fans are the examples.

For those applications which require higher dynamic performance than v/f control, the dc motor like control of IM that is called, the field oriented control (FOC) is preferred. During the last few years, a particular interest has been noted on applying speed sensorless FOC to high performance applications that is based on estimation of rotor speed by using the machine parameters, instantaneous stator currents and voltages [1]-[6]. The benefits of speed sensorless control are the increased reliability of overall system with the removal of mechanical sensors, thereby reducing sensor noise and drift effects as well as cost and size. However to exploit the benefits of sensorless control, the speed estimation methods must achieve robustness against model and parameter uncertainties over a wide speed range. To address this issue, a variety of approaches have been proposed.

The adaptive observers (AO) like Luenberger observer or the extended Kalman filter [1], [5] gets accurate estimates under detuned operating conditions but these solutions are computationally intensive, require more memory space and are difficult to tune because the initial values of three covariance matrices have to be assumed and selected after much trial and error. So their application in low cost drives is limited. The model reference adaptive system is also an AO technique [7], where the same quantity is calculated by two different ways. One of them is independent of variable to be estimated while the other one is dependent on it. The two computed quantities are used to formulate the error signal. The error signal is then fed to an adaptation mechanism which in most cases is a PI controller. The output of the adaptation mechanism is the estimated quantity.

While all the speed sensorless techniques eliminate the use of mechanical speed sensor, they require the stator current and stator voltage signals as input. This requires at-least two current sensors and two voltage sensors on the stator side. It is difficult to get current sensors with equal gains over the wide range of frequencies, voltages and currents used in a practical inverter. The problem is exacerbated if the motor windings are not perfectly balanced or if the current sensors have some dc offset. Over last few years, techniques of stator current reconstruction from the dc link current have been suggested in literature [8]-[9].

In this paper, a new speed sensorless control strategy for IM is proposed that includes the speed control, torque control and current regulation. Unlike conventional close loop estimators, it involves less computation and is less dependent on machine parameters. The stator currents and stator voltages are

reconstructed from dc link quantities and the inverter switching signals. For faithful reconstruction of currents, use of adaptable gain band-pass filter is proposed in the scheme. The simulation results of proposed scheme shows fast performance as compared to v/f control and therefore can be regarded as an improvement. For the close loop speed control, a single current sensor in the dc link is sufficient. Thus it is suitable for low-cost, moderate performance, sensorless IM drive applications. The proposed drive is modeled in Matlab/Simulink software for a 2.2 kW IM. The simulation results are presented to verify the workability of proposed strategy.

II. PROPOSED SCHEME

Fig. 1 shows the block diagram of the proposed scheme. It consists of a speed (frequency loop), a torque loop, and a current regulator. The output of speed/frequency regulator represents the torque reference for the torque loop. The torque Regulator generates the q-axis current command i_{qe}*.The d-axis current command i* qs is directly generated from the reference rotor flux ψ_r* as given by (1) [1]. This eliminates an additional PI controller and reduces the computational burden. These dc commands expressed in synchronously rotating reference after transformation to the three phase current commands are than compared with the actual three- phase currents (reconstructed waveforms) to generate the switching signals for the inverter. In the proposed scheme, all the feedback signals including the stator currents and stator voltages are estimated/reconstructed from the dc link quantities.

$$I_{dc}^{*} = \frac{\psi r}{Lm} \qquad (1)$$

III. RECONSTRUCTION OF STATOR VOLTAGES & CURRENTS FROM DC LINK

As indicated in [1], [6] ,the stator flux,torque and speed can be derived from the stator voltatges and currents expressed in d-q reference frame.The phase currents and voltages are related to the dc link current and voltage by inverter switching states.A coltage source inverter –IM drive is shown in Fig 2.where V_{dc} is the dc link voltage ,I_{dc} is the instantaneous dc link current and and i_a, i_b, i_c are the instantaneous three-phase winding currents.

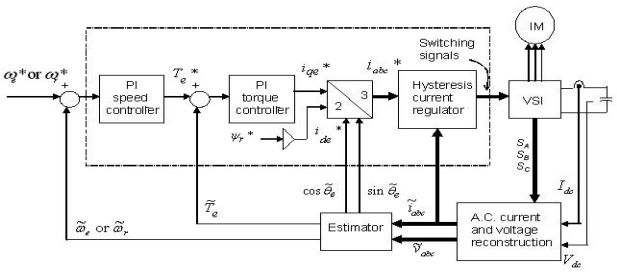

Figure 1. Block diagram of the proposed scheme.

. DC LINK CURRENT & PHASE VOLTAGES

Generally, IGBTs associated with snubber protection and feedback diode are used as switch in inverters. When a switch is being turned-on and the conducting diode at the same leg is being blocked off by this turn-on, because of the reverse recovery effect of the diode,this leg is shorted through . To establish the basic relationship between dc link current, winding currents and inverter switching pattern, the switches shown in Fig. 2 are considered as ideal; the diode recovery effect and the snubber action are not considered.

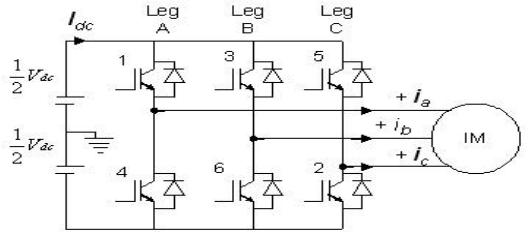

. Figure 2. Voltage source inverter fed induction motor drive

A. Space-Vectors

During normal state, there are eight switching states of inverter which can be expressed as space voltage vector (S_A,S_B,S_C) such as (0,0,0), (0,0,1), (0,1,0), (0,1,1), (1,0,0), (1,0,1), (1,1,0) and (1,1,1). S_A =1 means upper switch of leg A is on while the lower one is off, and vice versa. The same logic is applicable to S_B and S_C also. Amongst above eight voltage vectors, (0, 0,0) and (1,1,1) are termed as zero vectors while the other six as active vectors. The switching vectors describe the inverter output voltages.

B. Basic Principle of Phase Voltage & Line Current Reconstruction

For different voltage vectors, the phase voltage that will appear across stator winding can be determined by circuit the stator winding is star connected. From this table,the reconstructed expressions of three phase voltages are:

$$V_a = Vdc(2SA - SB - SC)/3 \qquad (2)$$

$$V_b = Vdc(-SA + 2SB - SC)/3 \qquad (3)$$

$$V_c = Vdc(-SA - SB + 2SC)/3 \qquad (4)$$

The stator voltages are expressed in stationary d-q frame are:

$$V_{qs}=V_a = Vdc(2SA - SB - SC)/3 \qquad (5)$$

$$V_{ds} = Vdc(SB - SC)/\sqrt{3} \qquad (6)$$

IV. Simulation Studies

In order to predict the behavior of the drive during steady-state and transient conditions, detailed simulation studies of the scheme shown in Fig.1 are carried out on a 2.2kW IM by using Simulink software. Fig. 3. shows the internal structure of the controller that consists of the speed loop, torque loop and the current regulation loop in synchronously rotating frame of reference. The switching signals for inverter are generated by comparing the command ac currents with reconstructed ac currents. For the reconstruction of stator voltages and ac line currents, the dc link quantities with V_{dc} = 600V are sampled with a sampling time of 2e-6 seconds and than segregated into the three-phase voltages and three ac currents as per (2)-(4) and (7)-(9) respectively. The simulation was carried out for five different operating conditions as is presented ahead. A variable- step ode23tb(stiff/TR-BDF2) solver was used. The waveforms of reconstructed phase voltages and the three ac line currents as reflected in the dc current, are presented in Fig.4. From these waveforms, it is clear that the samples of phase currents available in the dc link current are not evenly spread and being discontinuous, the set of resulting points do not constitute an acceptable reconstruction. Therefore a zero-order hold is employed followed by a band-pass filter. The

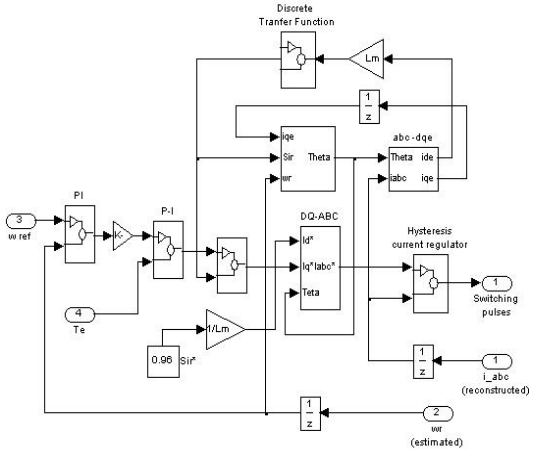

Figure 3. Simulink model of control strategy

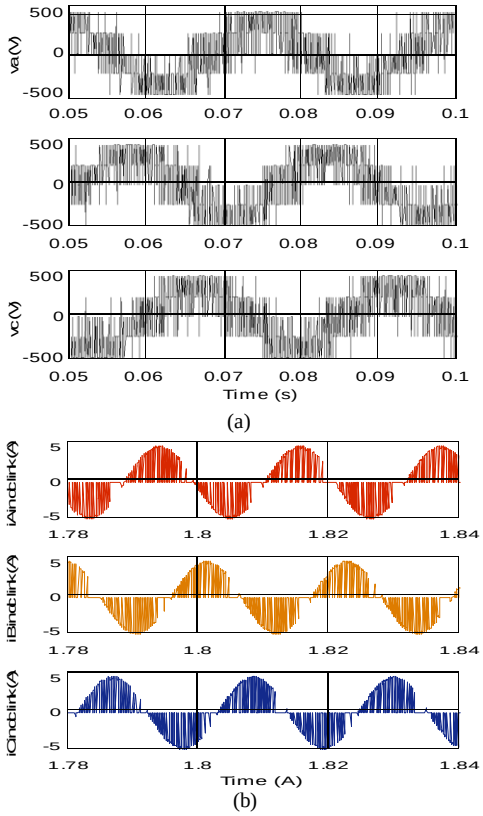

Figure 4. Reconstructed waveforms of (a) three phase voltages and (b) three line currents separated from the dc link current.

values of time constants T for the band-pass filter are selected by trial and error. The simulation output of band-pass filter which represents the reconstructed ac line currents is shown in Fig.5(a). For the sake of comparison, the actual ac line currents are illustrated in Fig.5(b). The reconstructed and actual waveforms of ac line currents during 100% speed reversal at no-load are presented in Fig.6(a) & (b). The response of speed sensorless drive during different

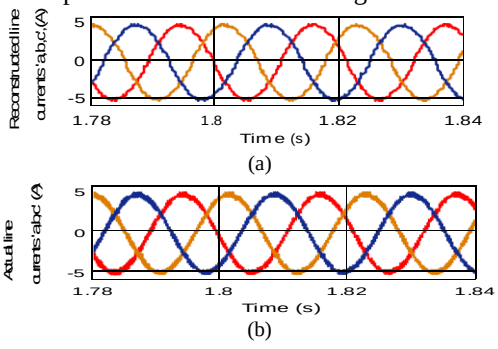

Figure 5. Stator currents at rated load (a) reconstructed (b) actual waveforms

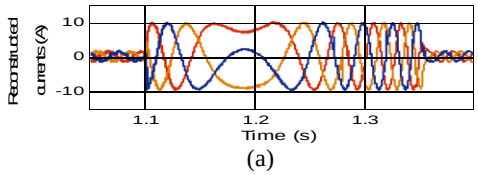

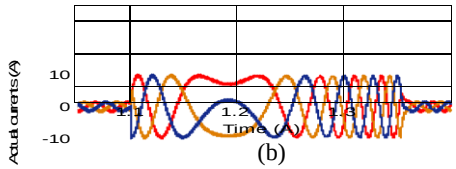

(b)

Figure 6. Stator currents during reversal at no-load (a) reconstructed waveform (b) actual waveform

dynamic conditions was studied in detail. To check the accuracy of estimated variables, these variables were obtained by two different methods. In the first one, the machine variables which include the flux, torque, synchronous-speed, slip-speed and rotor-speed are estimated by using (15)-(24) and in the second method, these variables are calculated with the help of dynamic model of IM [1] by using the stator currents and voltages measured directly. The simulation results of the first method were treated as estimated values while those of the latter method as actual values.

Case 1: Free acceleration characteristics:

The machine was allowed to accelerate from zero speed to rated speed at no-load. The steady-state was reached at 0.3 seconds. The waveform of estimated speed show faster response (less damped) as compared to its actual counterpart. This is shown in Fig. 7(a) & (b).

Case 2: Step change in speed reference:

Step change in speed reference was applied two times. At 0.5 sec., from +100% to +60% and vice-versa at 1 sec. was applied. The response is shown in Fig.8. The torque becomes negative during the first change to decelerate the motor. Upon reaching steady state, the torque becomes equal to the load torque. The response time of the drive for this step change is 100ms. The estimated values of torque and speed vary in accordance with their corresponding actual values.

Case 3: Speed reversal:

A step change in speed reference from +100% to -100% is applied at 1.5 seconds. This step change is equivalent to 100% speed change. The response is shown in Fig. 9. The phase sequence reverses to rotate the motor in reverse direction. The drive reaches steady state after the change in reference speed in 700 ms. this proves that the speed estimation is stable even at very low speeds.

Case 4: Step change in load:

A step change in load is applied at 0.5 seconds. The response of the drive is shown in Fig.10. The electromagnetic torque increases to correct the speed error. Upon reaching the steady state, the torque becomes equal to the load torque. The rotor speed, after an initial droop attains back its earlier speed . The motor reaches the steady state in 300ms.

Case 5: Low speed operation:

The response of the drive at 40% and 20% of rated speed is shown in Fig.11. For the machine under consideration, 20% corresponds to 3.14 rad/sec angular mechanical speed. The speed estimation is very stable even at this low speed range.

VII. CONCLUSION

In this paper, a new control strategy for induction motor drive is proposed. The drive is operated under torque control with an outer speed loop and is very similar to open-loop v/f drive in terms of power components and sensors required. Due to the inclusion of torque control loop, the drive response is fast and stable. Simulation results confirm the effectiveness of the proposed scheme. The technique uses only dc link voltage and dc link current measurements to generate the estimates of

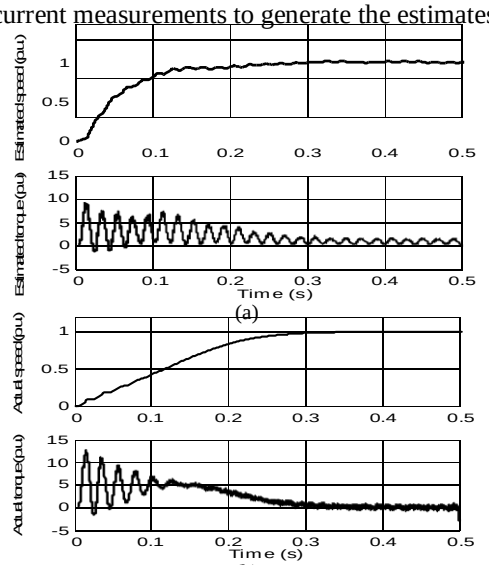

(a)
(b)

Figure 7. Free-acceleration characteristics (a) estimated & (b) actual values

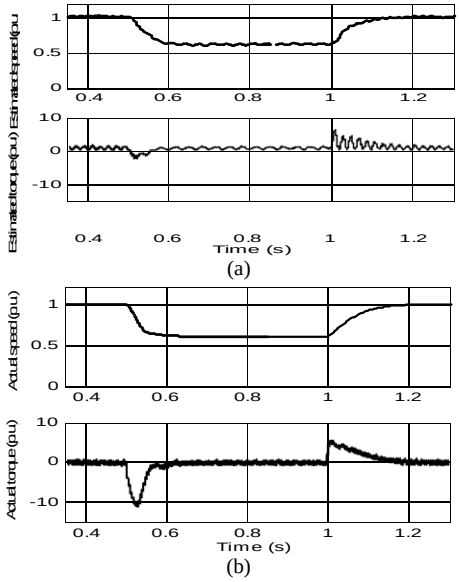

(a)
(b)

Figure 8. Variation in rotor speed and electromagnetic torque for step changes in reference speed (a) estimated values, (b) actual values

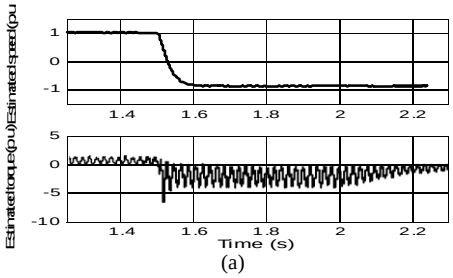

(a)

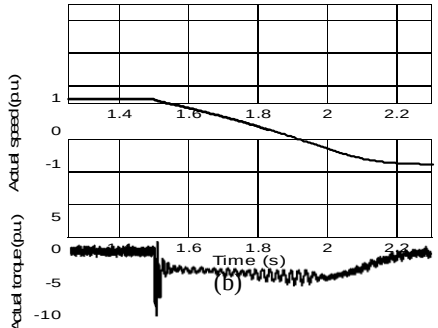

(b)

Figure 9. Variation in rotor speed and electromagnetic torque during reversal (a) estimated values, (b) actual values

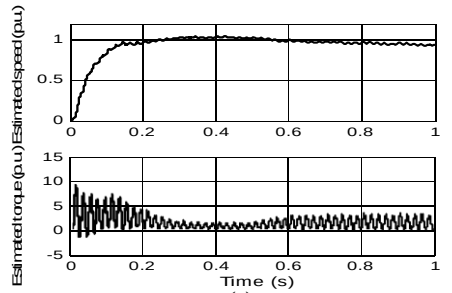

(a)

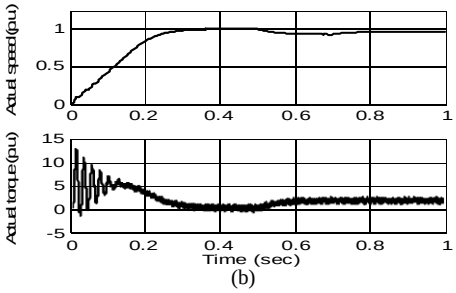

(b)

Figure 10. Variation in rotor speed and electromagnetic torque with step rise in load(a) estimated values, (b) actual values

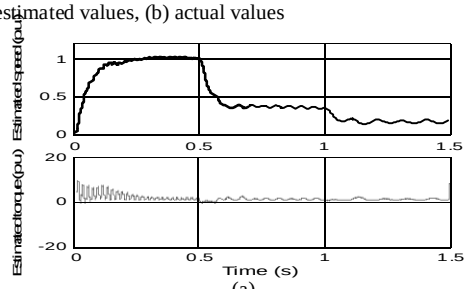

(a)

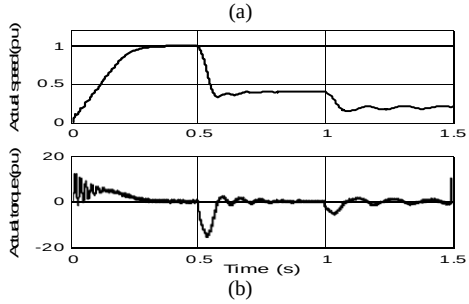

(b)

Figure 11. Variation in rotor speed and electromagnetic torque in low-speed region (a) estimated values, (b) actual values

phase voltages, line currents, flux, torque and rotor speed. If the dc link voltage is assumed as constant, only one current sensor in the dc link is sufficient to give the estimates of all required feedback variables. Moreover, the same current sensor that is already available in the dc link of an open-loop v/f drive for protection purpose can be used. Thus the open-loop control strategy in an existing v/f drive can be replaced by the proposed close-loop control strategy without requiring any additional power components or the physical sensors. The proposed strategy appears to be a good compromise between the high-cost, high-performance field-oriented drives and the low-cost, low-performance v/f drives.

Practical implementation of the proposed scheme on a 16 bits floating point arithmetic Texas Instrument TMS320C31 processor are the subject of future follow-up research work.

APPENDIX

MACHINE PARAMETERS

$R_s = 11.1\Omega;\ R'_r = 2.2605\Omega$
$L_s = 0.7329H;\ L'r = 0.7329H$
$L_m = 0.71469H;\ P = 4$

REFERENCES

[1] B. K. Bose, *Power Electronics and Motor Drives*, Delhi, India, Pearson Education, Inc., 2003.

[2] M. Rodic and K. Jezernik, "Speed-sensorless sliding-mode torque control of induction motor," *IEEE Trans. Ind. Electron*., vol. 49, no. 1, pp. 87-95, Feb. 2002.

[3] L. Harnefors, M. Jansson, R. Ottersten, and K. Pietilainen, "Unified sensorless vector control of synchronous and induction motors," *IEEE* pp. 153-160, Feb. 2003.

[4] M. Comanescu and L. Xu, "An improved flux observer based on PLL frequency estimator for sensorless vector control of induction motors," *IEEE Trans. Ind. Electron.*, vol. 53, no. 1, pp. 50-56, Feb. 2006.

[5] Radu Bojoi, Paolo Guglielmi and Gian-Mario Pellegrino, "Sensorless direct field-oriented control of three-phase induction motor drives for low-cost applications," *IEEE Trans. Ind. Appl.*, vol. 44, no. 2, pp. 475-481, Mar. 2008.

[6] I. Boldea and S. A. Nasar: Taylor& Francis, 2006.

[7] S. Maiti, C. Chakraborty, Y. Hori, and Minh. C. Ta, "Model reference adaptive controller-based rotor resistance and speed estimation techniques for vector controlled induction motor drive utilizing reactive power," *IEEE. Trans. Ind. Electron.* vol. 55, no. 2, pp. 594-601, Feb. 2008.

[8] B. Saritha and P. A. Janakiraman, "Sinusoidal three-phase current reconstruction and control using a dc-link current sensor and a curve-fitting observer," *IEEE Trans. Ind. Electron*., vol. 54, no. 5, pp. 2657-2662, Oct. 2007.

[9] H. Kim and T. M. Jahns, "Current control for AC motor drives using a single dc-link current sensor and measurement voltage vectors," *IEEE Trans. Ind. Appl*., vol. 42, no. 6, pp. 1539-1546, Nov./Dec. 2006.

[10] P. Vas, *Sensorless Vector and Direct Torque Control*, Oxford, U.K. Oxford Science, 1998.

[11] J. Zhao, B. K. Bose, "Neural-network-based waveform processing and delayless AC drives," *IEEE Trans. Ind. Electron*., vol. 51, no. 5, pp.981-991, Oct. 2004.